



HAL
open science

Buckling response of architected columns: controlling instability across the scales through a rational design.

Gabriella Tarantino, Matthieu Caruel, Kostas Danas

► To cite this version:

Gabriella Tarantino, Matthieu Caruel, Kostas Danas. Buckling response of architected columns: controlling instability across the scales through a rational design.. 13e colloque national en calcul des structures, Université Paris-Saclay, May 2017, Giens, Var, France. hal-01899349

HAL Id: hal-01899349

<https://hal.science/hal-01899349>

Submitted on 19 Oct 2018

HAL is a multi-disciplinary open access archive for the deposit and dissemination of scientific research documents, whether they are published or not. The documents may come from teaching and research institutions in France or abroad, or from public or private research centers.

L'archive ouverte pluridisciplinaire **HAL**, est destinée au dépôt et à la diffusion de documents scientifiques de niveau recherche, publiés ou non, émanant des établissements d'enseignement et de recherche français ou étrangers, des laboratoires publics ou privés.

Buckling response of architected columns: controlling instability across the scales through a rational design.

M.G. Tarantino¹, M. Caruel², K. Danas¹,

¹ LMS, Ecole Polytechnique, France, tarantino@lms.polytechnique.fr, kdanas@lms.polytechnique.fr

³ MSME, Université de Paris-Est, France, matthieu.caruel@u-pec.fr

Résumé — In the present study, we combine numerical simulations with compressive testing of 3D printed polymer structures to investigate the buckling response of a slender column, whose architecture employs unit-cell lattices which in turn consist of a sequence of columns uniformly spaced. The lower-scale columns are both of comparable size with the macro-geometry and *a priori* susceptible to buckling. Within the accuracy of data, the experimental trends are consistent with the numerical simulations and show that both the buckling and the post-buckling response at the macroscopic (i.e. continuum) level are dependent on the lower-scale microstructure.

Mots clefs — Instability, Bifurcation, Architected columns

1. Introduction

Man-made meta- materials and structures have received much attention over the past decades thanks to their aptitude for tailoring selected properties. Superior acoustic [1, 2], photonic [3] and mechanical [4, 5] properties can be deliberately achieved at the macroscale by rationally designing the structure's unit-cell geometry and level of hierarchy [6]. Hierarchical nanocomposites mimicking biological materials such as nacre, teeth and bone as well as cellular materials with periodic architecture are both examples of metamaterial systems.

All above material structures employ in their architecture two different, and often not comparable, length scales where the elementary building block is a few orders of magnitude smaller than the macrostructure. In such many cases, the bulk response of the solid/structure is determined by the response of a unit cell representative volume element (RVE) and numerical homogenization techniques can be exploited to determine the effective mechanical properties at a continuum level. Here, we explore whether homogenization theory holds its validity for predicting the response of hierarchical structures where there is no length-scale separation between the elementary unit cell and the macrostructure. To this end, we seek to design a 2-D model structure that allows a systematic investigation of the competition between length scales in triggering the mechanical response at a continuum level. Specifically, we investigate the buckling response of a slender column, whose architecture employs unit-cell lattices which in turn consist of a sequence of columns uniformly spaced. The lower-scale columns are both of comparable size with the macro-geometry and *a priori* susceptible to buckling.

In the present study, we combine numerical simulations with compressive testing of 3D printed polymer structures and show how a rational design of the column's architecture can control buckling instability across the scales.

2. Experimental section

2.1. Material and testing

In order to study the buckling response of architected columns experimentally, structures are designed, fabricated and tested. The structures were fabricated using Eden 260V 3D printer (Stratasys, France). A rubber-like flexible material, under the trade name *Tango Black*, was used for printing the structures. The chemistry of this material is proprietary to Stratasys. Prior to fabrication, the mechanical properties of the bulk material were determined by tensile testing of 3D-printed dog-bone specimens. The measured Young's modulus and Poisson's ratio of the bulk elastomer are respectively $E \approx 3 \text{ MPa}$ and $\nu \approx 0.499$. Note in passing that it was checked experimentally that 3D-printing produces solid specimens whose mechanical properties are found to be isotropic and therefore independent on the printing direction.

Geometries were prepared in a CAD software (SolidWorks 2016, Dassault Systèmes SolidWorks Corps., France) and then exported as Stereolithography files (i.e. STL format) for direct printing in the Object Eden 206V. Structures were jetted from designated nozzles in ultra-thin layers onto a build tray and each tiny droplet of liquid photopolymer was cured by UV light immediately after jetting, thus producing full cured specimens. The feature size that can be printed with sufficient accuracy by the Object Eden 260V printer is $\approx 500 \mu\text{m}$.

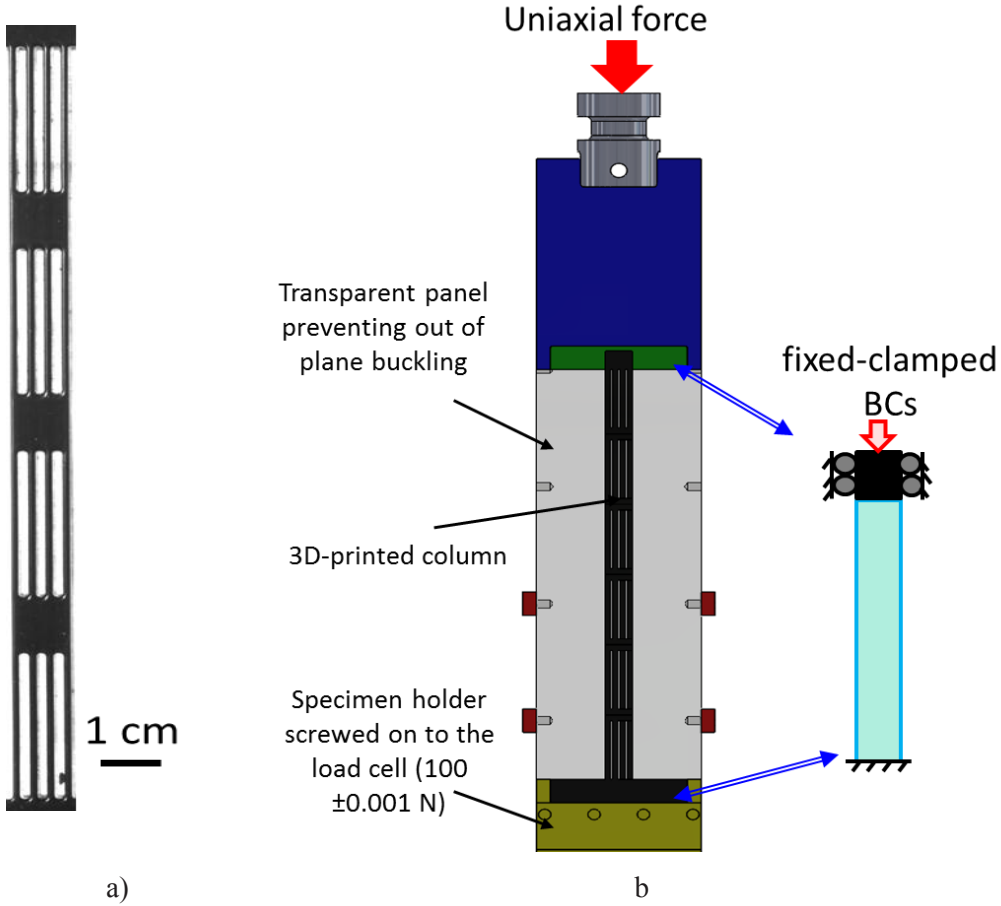


Figure 1: a) an example of a 3D-printed polymer column with a hierarchical architecture; b) compression testing device and methods.

Figure 1a shows an example of a 3D-printed structure used for this study. The column in Figure 1a consists of a vertical stack of four unit-cell lattices, where each elementary unit-block consists of an alternative stack of four columns uniformly spaced within the lattice. The connection of two sequential unit-cells in the vertical stack is ensured by thick spacers (see Figure 1a), that being nearly underformable can be regarded as rigid connectors. The slenderness ratio of each individual column in the unit-cell lattice is determined after fixing the unit-cell geometry (namely its thickness and height) and the solid volume fraction. Specifically, the structure depicted in Figure 1a features 50 vol. pct of solid phase (the latter being equally distributed among the four columns making the unit-cell).

Compression testing was then carried out onto as-fabricated structures using a MTS Hydraulic uniaxial machine (MTS Germany). Tests were conducted under displacement control at a crosshead speed of 0.005 mm/s. The load was measured with a $\pm 100\text{N}$ external force transducer mounted on the universal test rig, whereas high-resolution digital camera facing the specimen was used to collect images of the structure during its compressive deformation. Given the small axial forces applied onto the polymer structures, the crosshead displacement was used as measurement of the axial shortening of the structures. The specimen was enclosed within the fixed and movable platens of the universal testing machine and its upper and lower shoulders were rigidly clamped in order to prevent its rotation and horizontal sliding. Only axial shortening was allowed at the specimen upper end. A schematic of the compression testing methods is depicted in Figure 1b. Finally, in order to prevent out-of-plane buckling of the 3D-printed structures, transparent back plates were used to hold the specimen (Figure 1b).

3. Results and discussions

3.1. Experimental results

Experimental force vs. engineering strain curves are presented in Figure 2 a to b. For all structures tested (featuring 80 vol pct of solid phase), buckling of the columns making the elementary unit-cells is observed to trigger the macroscopic buckling. For the sake of clarity, hereinafter the term *micro* is used to refer to the scale of the elementary unit-cell and the slenderness ratio is defined as the ratio between the column's length and thickness.

Within the scatter of data, results are overall nicely reproducible and consistent. Specifically, Figure 2a shows the effect of the *micro*-slenderness ratio on the critical load of structures of identical *macro*-slenderness ratio. Comparing curves of solid squares and circle symbols indicates that decreasing the slenderness ratio of the columns in the unit-cell lattice (i.e. circles vs squares symbols in Figure 2a) is observed to increase the critical load of the architected column. The effect of the *macro*-slenderness ratio on the critical load of structures of identical *micro*-slenderness ratio is shown in Figure 2b. Increasing the macro-column slenderness (notably making the columns taller) decreases the critical load for buckling: if one compare curves of square, triangles and circles symbols (namely curves at increasing *macro*-slenderness ratios) one observes that the applied force necessary to make the structure buckle decreases.

Finally note in passing that, within the scatter of data, the post-buckling response seems to be affected by the competition between the length-scales (i.e. *micro* vs. *macro*). This is currently being investigated.

3.2. Numerical results

In order to investigate the problem further and therefore overcome the limitations of the structures that can be printed and tested, we have carried out in parallel a thorough numerical study. To this end, we have made an extensive use of finite element (FE) simulations within the commercial package ABAQUS/STANDARD to study both the buckling and post-buckling response of the architected structures featuring 80 vol pct of solid phase.

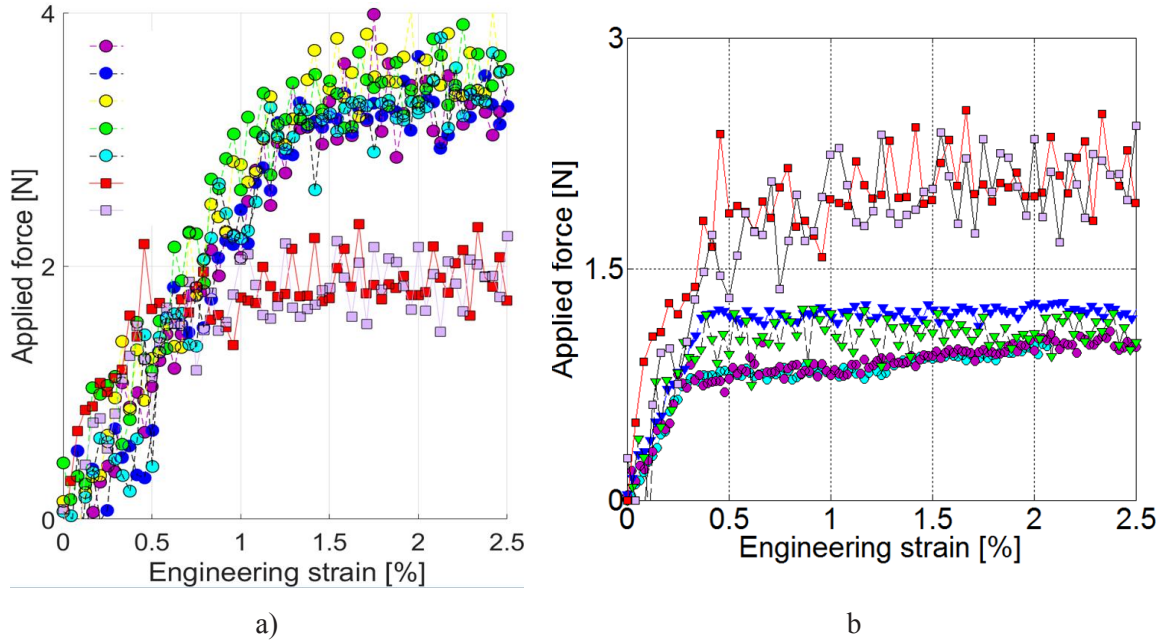


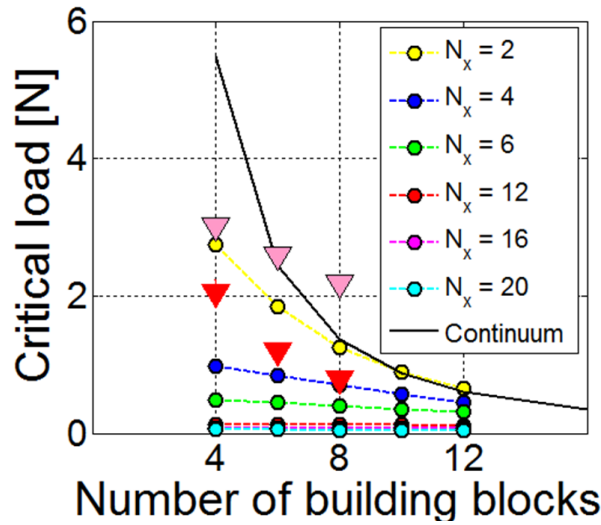
Figure 2 Experimental buckling response of 3D-printed hierarchical columns featuring 80 vol. pct of solid phase: a) effect of the increasing (i.e. solid circles) *micro*-scale slenderness ratio at equal *macro*-slenderness ratio; b) effect of the increasing (from solid squares to circles) *macro*-scale slenderness ratio at equal *micro*-slenderness ratio.

Since the rubber-like material used for fabricating the structures is well described by the incompressible neo-Hookean formulation of elasticity [6], 2D numerical simulations with linear plane strain hybrid elements (ABAQUS element type CPE4H) were performed and the experimentally measured Young’s modulus and Poisson’s ratio (see Section 1.1) were used to define the material properties. Furthermore, given the regularity of the geometries, the mesh was constructed by means of a custom-made code in *Matlab* language.

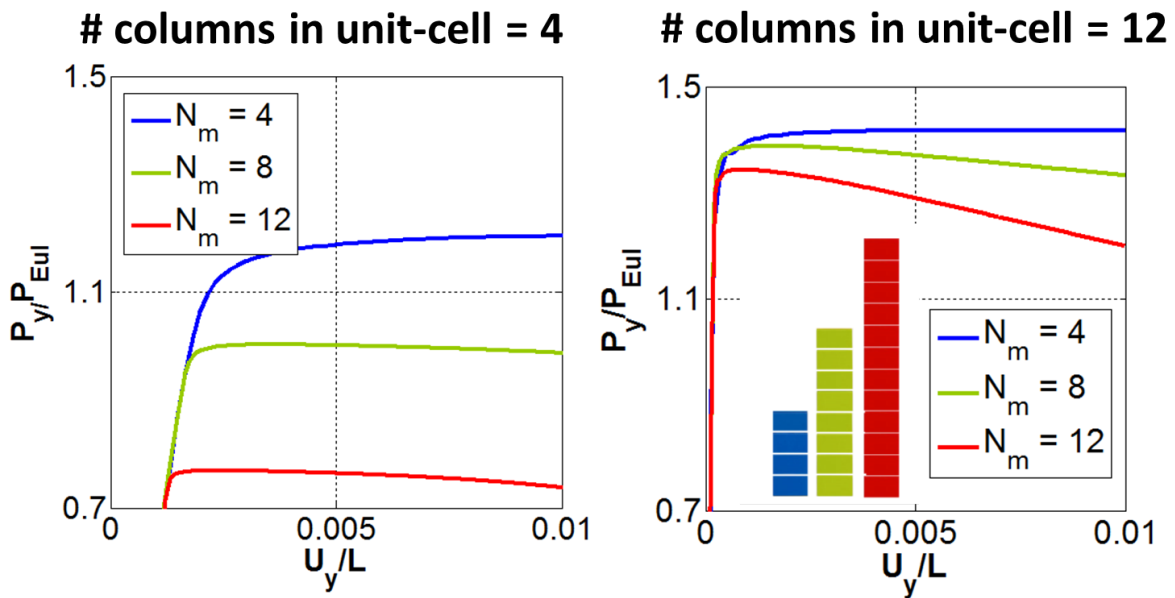
Two types of numerical analyses were conducted: (i) a linear BUCKLE type analysis and (ii) a quasi-static perturbation analysis including non-linear geometrical effects. Both types of FE analyses were carried out with the purpose of investigating systematically how the competition between *micro*- and *macro*- instabilities affects respectively (i) the critical buckling loads and corresponding deformation modes and (ii) the post-buckling response. For the latter type of analysis, a combined imperfection given by the superimpositions of first three buckling modes (determined by a linear buckling analysis) was introduced. The imperfection amplitude was taken equal to 0.1% of the macro-column thickness.

The results of the numerical simulations are depicted in Figure 3. Specifically, Figure 3a shows the effect of increasing *macro*-slenderness ratio (i.e. increasing number of elementary building blocks N_m) at equal *micro*-slenderness ratio (i.e. at equal number of columns N_x in the unit-cell). Note that, in

Figure 3a the solid black line represents the theoretical continuum approximation given by the Euler critical load. The results of the linear BUCKLE analysis indicate that: (i) at increasing *micro*-slenderness ratio, the critical loads changes less rapidly with increasing *macro*-slenderness ratio (e.g. compare yellow and cyan curves); (ii) at equal *macro*-scale slenderness ratio, $P \rightarrow 0$ for $N_x \rightarrow \infty$ thereby indicating that the continuum approach is far from predicting buckling and (iii) there is a tendency for $P \rightarrow 0$ regardless the *micro*-scale slenderness ratio for an infinite slenderness column. Furthermore, comparing the numerical results (dotted lines yellow and blue) with (i) the experimental measurements to date (the latter are represented by solid pink (i.e. $N_x = 2$) and red (i.e. $N_x = 4$) triangles) shows fairly good agreement.



a)



b)

Figure 3 Numerical simulations of the buckling response of 3D-printed hierarchical columns featuring 80 vol. pct of solid phase; a) the linear BUCKLE analysis results and b) quasi-static perturbation analysis simulations including non-linear geometrical effects.

On the other hand, curves of the applied load normalized by the Euler load for the column vs. axial compressive deformation are presented in Figure 3b. Comparing curves of identical color in Figure 3b shows that at equal *macro*-slenderness ratio (i.e. N_m) the post-buckling response is dependent on lower-scale microstructure, namely the *micro*-slender ratio.

4. Conclusions

We have studied buckling instability of architected columns. The study combines numerical simulations with compressive testing of 3D printed polymer structures. Results to date show that:

- Lower scale micro-structure is found to trigger instability at the *macro*-scale, the latter being characterized by long- and short-waviness;
- Within the accuracy of data to date, experimental trends are consistent with the numerical results;
- The macroscopic critical load is microstructure dependent and a continuum approach is observed to yield predictions far from experimental and numerical values.

Références

- [1] Lu, M. H., Feng, L., & Chen, Y. F. (2009). Phononic crystals and acoustic metamaterials. *Materials Today*, 12(12), 34-42.
- [2] Brunet, T., Merlin, A., Mascaro, B., Zimny, K., Leng, J., Poncelet, O., & Mondain-Monval, O. (2015). Soft 3D acoustic metamaterial with negative index. *Nature materials*, 14(4), 384-388.
- [3] Soukoulis, C. M., & Wegener, M. (2011). Past achievements and future challenges in the development of three-dimensional photonic metamaterials. *Nature Photonics*, 5(9), 523-530.
- [4] Lee, J. H., Singer, J. P., & Thomas, E. L. (2012). Micro-/Nanostructured Mechanical Metamaterials. *Advanced materials*, 24(36), 4782-4810.
- [5] Babaei, S., Shim, J., Weaver, J. C., Chen, E. R., Patel, N., & Bertoldi, K. (2013). 3D Soft metamaterials with negative Poisson's ratio. *Advanced Materials*, 25(36), 5044-5049.
- [6] Wang, L., Lau, J., Thomas, E. L., & Boyce, M. C. (2011). Co- Continuous composite materials for stiffness, strength, and energy dissipation. *Advanced Materials*, 23(13), 1524-1529.